Single-cell analysis reveals the *KIT* D816V mutation in hematopoietic stem and progenitor cells in systemic mastocytosis

Short title: Single-cell mutation analysis in mastocytosis

Jennine Grootens[1], Johanna S. Ungerstedt[2,3], Maria Ekoff[1], Elin Rönnberg Höckerlind[1], Monika Klimkowska[4], Rose-Marie Amini[5], Michel Arock[6], Stina Söderlund[7,8], Mattias Mattsson[5,7], Gunnar Nilsson[1,7,8], and Joakim S. Dahlin[1]

Author affiliations:
[1]Department of Medicine Solna, Karolinska Institutet, and Karolinska University Hospital, Stockholm, Sweden;
[2]Department of Medicine Huddinge, Karolinska Institutet, Stockholm, Sweden;
[3]Hematology Center, Karolinska University Hospital, Stockholm, Sweden;
[4]Department of Clinical Pathology and Cytology, Karolinska University Hospital Huddinge, Stockholm, Sweden;
[5]Department of Immunology, Genetics and Pathology, Uppsala University, Uppsala, Sweden;
[6]Molecular and Cellular Oncology, Ecole Normale Supérieure de Cachan, Cachan, France and Clinical Hematology Laboratory, Pitié-Salpêtrière Hospital, Paris, France;
[7]Division of Hematology, Uppsala University Hospital, Uppsala, Sweden;
[8]Department of Medical Sciences, Uppsala University, Uppsala, Sweden

Address correspondence to:
Gunnar Nilsson, Department of Medicine, Immunology and Allergy unit, Karolinska Institutet, SE-171 76 Stockholm, Sweden; e-mail: gunnar.p.nilsson@ki.se
or
Joakim Dahlin, Department of Medicine, Immunology and Allergy unit, Karolinska Institutet, SE-171 76 Stockholm, Sweden; e-mail: joakim.dahlin@ki.se

Abstract word count: 239
Text word count: 3604
Number of figures: 6
Number of tables: 1

35 Number of references: 37

36

37 Key points:

38 • Single-cell analysis reveals the *KIT* mutation in hematopoietic stem and
39 progenitor cells and its accumulation in mast cells of SM patients

40 • CD45RA is a specific marker for aberrant mast cells in SM

41

Abstract

Systemic mastocytosis (SM) is a hematological disease characterized by organ infiltration by neoplastic mast cells. Almost all SM patients have a mutation in the gene encoding the tyrosine kinase receptor KIT causing a D816V substitution and autoactivation of the receptor. In this study, we analyzed the occurrence of the D816V mutation during hematopoiesis to evaluate whether this mutation is an early or late event in SM. Using a panel of 9 fluorescently labeled antibodies, 10 different hematopoietic progenitor subsets and mature mast cells were identified. The frequencies of the progenitor subsets did not differ between controls and SM patients. Single-cell index sorting and D816V mutation assessment were applied to analyze mast cells and more than 10,000 $CD34^+$ bone marrow progenitors from SM patients. We found that in SM 60-99% of the mast cells harbored the mutation, and the mutation could be detected throughout the hematopoietic landscape, from stem cells to more lineage-primed progenitors. However, the occurrence of the mutation in stem and progenitor cells was heterogeneous and varied between patients. Thus, the D816V mutation appears to be an early event in the development of SM but accumulates in the mast cell lineage. In addition, we demonstrate that mast cells originate from an $Fc\varepsilon RI^+$ bone marrow progenitor, and we describe aberrant CD45RA expression on SM mast cells for the first time. Taken together, our findings provide novel insight into hematopoiesis and the occurrence of the *KIT* D816V mutation in SM.

63 **Introduction**

64 Hematopoietic stem cells (HSCs) in the bone marrow give rise to all blood cells,
65 including mast cells. Differentiating HSCs progress through a number of intermediate
66 progenitors with multilineage-forming capacity before commitment to the mast cell
67 lineage.[1,2] The binding of stem cell factor (SCF) to its receptor, KIT, promotes the
68 maturation and proliferation of mast cells.[3-6] It is therefore not surprising that
69 mutations in the *KIT* gene coincide with the mast cell-driven disease systemic
70 mastocytosis (SM).[7]

71

72 SM is a hematologic neoplasm in which infiltrates of neoplastic mast cells occur in
73 various tissues.[8,9] The majority of SM patients carry a mutation in *KIT*, most
74 commonly affecting codon 816.[10] The *KIT* D816V mutation makes receptor signaling
75 constitutively active, independent of binding to its ligand SCF. The detection of *KIT*
76 D816V in either bone marrow or peripheral blood samples is one of the criteria for the
77 clinical diagnosis of SM using a standardized qPCR assay.[11] When the *KIT* D816V
78 mutation is present in mast cells, it may also be detected in mature bone marrow or
79 peripheral blood cells, such as basophils, eosinophils, neutrophils, and B and T
80 lymphocytes, which depends on the patient.[12-17] Furthermore, the precursors of
81 erythroid and myeloid cells as well as $CD34^+$ progenitors may carry the *KIT* D816V
82 mutation.[12,18,19] Taken together, these findings suggest that the mutation may arise in
83 early hematopoietic stem and progenitor cells (HSPCs), rather than in a lineage-
84 restricted precursor.

85

86 The $CD34^+$ cell compartment is highly heterogeneous, spanning HSCs to late lineage-
87 committed progenitors. In the present study, we delineated the cellular origin of the

88 *KIT* D816V mutation in single bone marrow cells in SM by combining FACS index
89 sorting of $CD34^+$ HSPCs with a multiplex qPCR assay. The data revealed that the
90 D816V mutation in *KIT* arises in early HSPCs. The mutation burden is low but
91 variable in multipotent and lineage-restricted progenitor populations and increases in
92 mature mast cells. Furthermore, the present study provides more insight into
93 hematopoiesis in SM subjects and reveals a novel marker for aberrant mast cells.
94
95 **Patients, materials, and methods**
96
97 *Patients and sample preparation*
98 Bone marrow and occasional peripheral blood samples were collected from patients
99 under evaluation for SM and from control subjects. The study was approved by the
100 Stockholm and Uppsala Regional Ethics committee. Oral and written informed
101 consent was obtained from each patient and control subject. The study was conducted
102 in accordance with the World Medical Association Declaration of Helsinki. The
103 patients included in our experimental studies were classified according to the World
104 Health Organization criteria[20] as having indolent SM (ISM, n = 19), aggressive SM
105 (ASM, n = 3), SM with associated hematological neoplasm (SM-AHN, n = 3), or
106 other malignancies, including myelodysplastic syndrome or myeloproliferative
107 neoplasm (MDS or MPN, n = 2). Table S1 shows the patient characteristics. For
108 analytic purposes, ASM and SM-AHN patients were combined in an advanced SM
109 group (AdvSM). The controls (Ctrl) included patients with cutaneous mastocytosis
110 (CM, n = 2) and subjects without SM (n = 7). All samples were processed on the day
111 of collection. Red blood cells were lysed with PharmLyse buffer (BD Biosciences,

112 Franklin Lakes, NJ) and washed with PBS containing 2% fetal calf serum (FCS,
113 Thermo Fisher Scientific, Waltham, MA).
114
115 *Cell lines*
116 Two human mast cell lines, HMC-1.2 and ROSA$^{KIT\ WT}$, with and without the *KIT*
117 D816V mutation, respectively, were cultured as previously described.[21,22]
118
119 *Flow cytometry and cell sorting*
120 Bone marrow cells were stained with fluorophore-conjugated monoclonal antibodies
121 in Brilliant Stain Buffer (BD Biosciences, Franklin Lakes, NJ). The antibodies used
122 for staining included CD10 (HI10a), CD14 (M5E2), CD34 (581), CD38 (Hb7),
123 CD45RA (HI100), CD90 (5E10), CD117 (104D2), CD123 (6H6), CD133 (AC133),
124 and FcεRIα (CRA-1) (all from BD Biosciences, Biolegend, San Diego, CA, or
125 Miltenyi Biotec, Bergisch Gladbach, Germany). The live/dead cell marker DAPI (BD
126 Bioscience) was used for the analysis of cultured cells. Cell sorting and analysis were
127 performed using the FACSAria III and LSRFortessa systems (BD Biosciences). For
128 cell culture experiments, cells were sorted into sterile-filtered PBS with 2% FCS
129 following a two-step sorting protocol, using the yield followed by the purity precision
130 mode. The analysis of 20-100 sorted cells verified the sorting purity. Single CD34^{+}
131 cells were sorted into 2 µl of lysis buffer containing 20 µg/ml PCR-grade proteinase K
132 (Thermo Fisher Scientific) in EB buffer (Qiagen, Hilden, Germany). These cells were
133 sorted either immediately from the sample or following an enrichment sort. The
134 single-cell precision mode ensured that only one cell was deposited per well. The
135 plates were then centrifuged and stored at -80°C until analysis. The sorting data from
136 single cells were saved using the index sort module of the software FACSDIVA

137 software version 8 (BD Biosciences). Flow cytometry data analysis was performed
138 using FlowJo software version 10 (TreeStar, Ashland, OR).
139
140 *Cell culture and colony-forming assays*
141 Colony-forming potential was evaluated by plating 500 cells in 35 x 10 mm tissue
142 culture dishes (Thermo Fisher Scientific) in duplicate. The cells were cultured in
143 Methocult H4434 (STEMCELL Technologies Inc., Vancouver, Canada). Colonies
144 were counted after 12-13 days, distinguishing erythroid, granulocyte/monocyte, and
145 mixed colonies following the manufacturer's recommendations. The mast cell-
146 forming potential was assessed via liquid culture as described previously.[23] Briefly,
147 sorted cells were cultured in medium with recombinant human (rh) IL-3 (10 ng/mL;
148 PeproTech, Rocky Hill, NJ) and rhIL-6 (10 ng/mL; PeproTech). In some experiments,
149 the medium was changed on day 5, and the cells were subsequently cultured with
150 rhIL-6 (10 ng/mL) and SCF (100 ng/mL, r-metHuSCF; Swedish Orphan Biovitrum,
151 Stockholm, Sweden), as indicated in the figure legends. Enzyme cytochemical
152 staining of trypsin-like activity was used to assess tryptase expression.[24,25] Cell
153 morphology was evaluated by May-Grünwald Giemsa staining (MGG; Sigma-
154 Aldrich, St. Louis, MO).
155
156 *Single-cell mutation analysis*
157 Before the addition of lysis buffer, 96-well plates (Bio-Rad Laboratories, Hercules,
158 CA) were UV-treated for 30 minutes using a UVT-B-AR UV Cabinet (Grant
159 Instruments, Cambridge, UK). Tubes and pipettes were treated with the DNA AWAY
160 Surface Decontaminant (Thermo Fisher Scientific). After sorting, the cells were lysed
161 for 45 minutes at 55°C, followed by a 10-min heat-inactivating step at 95°C.

162 Multiplex qPCR analysis was performed via a Taqman gene expression assay
163 (Thermo Fisher Scientific) in lysed single cells using 96-well CFX Manager (Bio-Rad
164 Laboratories). A mutation assay was designed based on a previously published
165 method[11] using Primer3 (v.0.4.0) which specifically detected *KIT* D816V using the
166 forward primer 5'-AGAGACTTGGCAGCCAGAAA-3'; a reverse primer matching
167 the mutation at the 3' position, 5'-
168 TTAACCACATAATTAGAATCATTCTTGATGA-3'; and the probe 5'-FAM-
169 TCCTCCTTACTCATGGTCGGATCACA-BHQ1-3'. A control assay was designed
170 to target a flanking exon and intron eight in GAPDH using the forward primer 5'-
171 CTGACTTCAACAGCGACACC-3'; the reverse primer 5'-
172 AGAGTTGTCAGGGCCCTTTT-3'; and the probe 5'-HEX-
173 TCAAGCTCATTTCCTGGTATGTG-BHQ1-3' (all primers came from TAG
174 Copenhagen, Denmark). The control and mutation assays were tested and optimized
175 using the cell lines ROSA$^{KIT\ WT}$ and HMC-1.2. The primer concentrations, optimized
176 for single cells, were as follows; control assay 150 nM forward/reverse primers, 100
177 nM probe; mutation assay 100 nM forward/reverse primers, 67 nM probe. Each plate,
178 containing 86 CD34^{+} cells, 5 mature mast cells, 3 empty wells, and 2 wells with bulk
179 CD34^{+} cells following sorting, was subjected to the multiplex qPCR assay. Cells were
180 excluded from analysis when amplification failed in the control assay, or when
181 amplification of the control assay resulted in a CT value higher than 40. In the
182 mutation assay, cells were regarded as unmutated when there was no amplification or
183 when the CT value was higher than 45. Outliers from each plate were then detected
184 using the ROUT outlier test in Prism software and removed from further analyses
185 (Figure S5B). Plates and cells that passed the quality control procedure were linked
186 with the index data and gated similarly to the whole sample for analysis.

187

188 *Statistical analysis*

189 Statistical analysis was performed using Prism software (Version 6.0h, GraphPad
190 Software, La Jolla, CA). The unpaired two-tailed Student's t-test was employed when
191 comparing two groups, and the unpaired one-way ANOVA with Tukey's multiple
192 comparison test was employed when comparing more than two groups. Statistical
193 analysis of log-transformed data was performed for some experiments as indicated in
194 the figure legends. Differences were considered significant when $P < .05$.

195

196 For original data, please contact joakim.dahlin@ki.se

197

198 **Results**

199

200 *Systemic mastocytosis patients have a normal CD34$^+$ bone marrow stem and*
201 *progenitor cell composition*

202 To assess the composition of the hematopoietic cells in the bone marrow of SM
203 patients, we designed a multicolor flow cytometry panel that identifies ten distinct
204 HSPC subtypes and mature mast cells (Table 1; Figures 1A-B). Colony formation
205 assays confirmed the validity of the GMP, CMP, and MEP gating strategies in SM
206 subjects (Figure S1A-C). The flow cytometry data provided a specific HSPC profile
207 for 34 bone marrow samples: 9 control, 19 ISM and 6 AdvSM (Table S1; Figure 1C).
208 The percentages of HSPCs in SM samples did not significantly differ from those in
209 control samples (Figures 1D and S2A). In addition, the ISM and AdvSM samples
210 exhibited percentages of total CD34$^+$ cells similar to the control samples (Figure

211 S2B). Thus, the overall hematopoiesis profile did not differ between the control and
212 SM subjects.
213
214 *The bone marrow CMP$^{Fc\varepsilon RI+}$ fraction presents an enhanced mast cell-forming*
215 *potential*
216 Mast cell progenitors circulate in the blood as Lin^{-} CD34^{hi} CD117$^{int/hi}$ FcεRI^{+} cells.[33]
217 These cells express CD123 and lack CD45RA,[23,33] overlaying the CMP$^{Fc\varepsilon RI+}$ gate in
218 bone marrow (Figure S3A). We therefore analyzed the mast cell-forming potential of
219 the bone marrow CMP$^{Fc\varepsilon RI+}$ fraction by culturing the cells with IL-3 and IL-6. Flow
220 cytometry analysis revealed that the CMP$^{Fc\varepsilon RI+}$ cultures gave rise to a higher
221 frequency of CD117^{hi} FcεRI^{+} mast cells than the CMPs$^{Fc\varepsilon RI-}$ cells (Figures 2A-C),
222 despite overall lower CD117 expression (Figure S4A). May-Grünwald Giemsa and
223 enzymatic tryptase staining showed that the CMP$^{Fc\varepsilon RI+}$ progeny generated a high
224 frequency of granulated tryptase-positive mast cells when cultured with SCF (Figures
225 2D-E and S3B). Cultured GMPs did not give rise to any cells with a mast cell
226 phenotype (Figure S3C).
227
228 The emerging model of hematopoiesis proposes that MEPs, basophils, and
229 eosinophils develop separately from GMPs following an asymmetric cell division at
230 the MPP stage. This process can be traced by the segregation of CD133, which is
231 expressed in GMPs but not in progenitors with erythromyeloid output.[34] Indeed, we
232 found that CMP$^{Fc\varepsilon RI+}$ cells lacked CD133 staining, similar to erythromyeloid cells
233 (Figure S4B).
234
235 *CD45RA is expressed on aberrant mast cells in systemic mastocytosis*

236 The multicolor flow cytometry panel used for the gating of HSPCs was also employed
237 to identify mast cells in bone marrow (Figure 1B). May-Grünwald Giemsa and
238 tryptase staining confirmed that $CD14^-$ $CD34^-$ $CD117^{hi}$ $Fc\varepsilon RI^{hi}$ cells constitute mast
239 cells (Figure 3A). SM samples presented higher percentages of mast cells than
240 controls (Figure 3B). Notably, mast cells from almost all SM samples exhibited
241 aberrant CD45RA expression, as verified with fluorescence minus one control and
242 internal control staining of $CD34^+$ cells (Figures 3C-D). The cutaneous (non-
243 systemic) mastocytosis samples and MDS/MPN samples lacked expression of
244 CD45RA on bone marrow mast cells (Figures 3C-D). In addition, mast cell
245 frequencies were correlated with the clinical percentage of BMMC infiltrate and
246 serum tryptase levels (Figures 4A-C; Table S2). Taken together, the results indicate
247 that SM bone marrow samples contain more mast cells than control samples and these
248 mast cells express the aberrant marker CD45RA.
249
250 *Single-cell index sorting reveals the KIT D816V mutation in early HSPCs in systemic*
251 *mastocytosis patients*
252 The cellular origin of the *KIT* D816V mutation in SM has not been established, and
253 the relative abundance of this mutation in different $CD34^+$ HSPC populations and
254 mast cells has not been determined. We therefore developed a single-cell method to
255 trace the *KIT* D816V mutation using two cell lines: HMC-1.2 cells carrying the
256 mutation and ROSA cells carrying wild-type *KIT*. The cells were labeled with two
257 different fluorochrome-labeled antibodies, mixed, and randomly FACS sorted with
258 the index sort function. A multiplex qPCR assay was used to detect an irrelevant gene,
259 for quality control purposes, and the *KIT* D816V mutation (Figure S5A-B). Among all
260 single cells, more than 96% passed the quality control procedure (Figure S5C).

261 Linking the results with the index data revealed that the mutation assay was negative
262 for the wild-type ROSA cells. The assay detected the mutation in 98.1% of all HMC-
263 1.2 cells. Thus, the assay did not detect false positive cells in the mutation assay and
264 only a few false negatives, demonstrating the high sensitivity and specificity of the
265 method (Figure S5D).
266
267 The high success rate with cell lines allowed us to use the assay for HSPCs and
268 mature mast cells from patient samples. Single cells from 12 samples (6 ISM and 6
269 AdvSM) were analyzed for mutation assessment. Specifically, $CD34^+$ HSPCs were
270 index sorted from ten patients, whereas specific HSPC subsets were sorted from two
271 patients. At the time of SM diagnosis, the presence of the *KIT* D816V mutation was
272 confirmed in either peripheral blood or bone marrow (Table S1). We analyzed 40-194
273 single mast cells and 351-1583 single $CD34^+$ cells from each bone marrow sample,
274 providing mutation data for 12,859 single cells in total (Figure 5A; Table S3). All SM
275 samples carried the *KIT* D816V mutation in the mast cell compartment at a high
276 frequency in ISM (mean, 80.9%) and AdvSM (mean, 93.2%) (Figure 5B). The
277 percentage of mutated mast cells was correlated with the total percentage of mast cells
278 in the sample and with the serum tryptase levels (Figure 6A-B; Table S2). The
279 mutation rate in $CD34^+$ HSPCs was less than 2.7% in all samples (Figure 5C), except
280 for one advanced SM sample with a high mutation burden of 37.0% (Table S4).
281 Nevertheless, the percentage of mutated $CD34^+$ HSPCs was correlated with serum
282 tryptase levels (Figure 6C; Table S2).
283
284 Coupling the index data with the mutation analysis of 10 bone marrow samples
285 revealed that the *KIT* D816V mutation appeared throughout the hematopoietic

286 landscape (Figure 5D; Table S3-4). Specifically, different HSPCs presented similar
287 mutation rates in all samples when the median percentage of mutation was compared
288 between different HSPCs (Figure 5E). Overall, the method of index sorting provided a
289 representative set of single cells from the whole-bone-marrow aspirates (Figure S6A).
290 However, the $CMP^{Fc\varepsilon RI+}$ population with an enriched mast cell potential was rare. To
291 determine the mutation frequency in the $CMP^{Fc\varepsilon RI+}$ fraction, we selectively sorted 86
292 and 278 single $CMPs^{Fc\varepsilon RI+}$ from 2 SM samples. One patient exhibited less than 2%
293 mutated $CMPs^{Fc\varepsilon RI+}$, HSCs and GMPs, whereas the fraction of mutated mast cells was
294 98.9% (Figure 5F; Table S4). The second patient presented 95.7% mutated
295 $CMPs^{Fc\varepsilon RI+}$ and 96.4 % mutated mast cells. (Figure 5G; Table S4). Peripheral blood
296 MCPs ($CD14^-$ $CD34^+$ $CD117^+$ $Fc\varepsilon RI^+$) showed mutation rates comparable to that of
297 bone marrow $CMPs^{Fc\varepsilon RI+}$ in one patient (Figure S6B), but the mutation could not be
298 detected in the MCPs from 4 other SM samples, likely due to the low mutation
299 frequency and the small number of cells analyzed due to the rarity of the cells (14-23
300 cells analyzed per sample). Taken together, we detected the *KIT* D816V mutation
301 throughout the hematopoietic landscape, starting with the HSCs.
302

303 **Discussion**

304 The cellular origin of the aberrant clone in SM is still under debate. Here, we show
305 that SM patients exhibit an increased frequency of mast cells in bone marrow. Almost
306 all these mast cells carry the *KIT* D816V mutation. Despite normal HSPC frequencies
307 in bone marrow, the *KIT* D816V mutation can be traced all the way back to the
308 $CD34^+$ $CD38^-$ $CD10^-$ $CD45RA^-$ $CD90^+$ HSC fraction.
309

310 The *KIT* D816V mutation causes receptor autoactivation, which signals survival,
311 proliferation, and differentiation, likely explaining the competitive growth advantage
312 of the aberrant mast cell clone and the high frequency of mutated mast cells.
313 However, the frequency of mutated HSPCs was low in most patients. This
314 observation is consistent with the overall normal HSPC composition of SM patients.
315 There are two main potential explanations for the low D816V mutation burden
316 observed in HSPCs and its accumulation in mast cells: HSPCs rapidly differentiate
317 into mast cells when the mutation occurs, or mutated HSPCs do not present a strong
318 growth advantage over non-mutated HSPCs. In fact, we have previously shown that
319 KIT signaling is dispensable for mast cell progenitor development, and that other
320 stimuli can induce cell proliferation.[23] However, the aberrant progenitor clone may in
321 some cases proliferate to reach a high frequency, as demonstrated in two patients with
322 advanced SM who presented more than 20% mutated cells in the HSC fraction.
323 Advanced forms of SM have previously been associated with detection of the *KIT*
324 mutation in bulk-sorted $CD34^{+}$ progenitors and various mature cell lineages, whereas
325 in indolent disease, the mutation is mainly restricted to mast cells.[13]
326
327 It is of particular interest to study the mutation burden in progenitors with mast cell-
328 forming potential. We have previously reported that $CD34^{+}$ $CD117^{int/hi}$ $Fc\varepsilon RI^{+}$ cells in
329 peripheral blood are committed or nearly committed MCPs.[33] Considering the $CD34^{+}$
330 $CD117^{+}$ $Fc\varepsilon RI^{+}$ phenotype of $CMPs^{Fc\varepsilon RI+}$ cells, these cells might be expected to
331 present a similar mast cell-forming capacity as to blood MCPs. In the current study,
332 we showed that $CMPs^{Fc\varepsilon RI+}$ gave rise to a higher frequency of mast cells than
333 $CMPs^{Fc\varepsilon RI-}$ and GMPs. However, the mast cell frequency in cultured $CMPs^{Fc\varepsilon RI+}$ was
334 less than 10% and a substantial fraction were found to be $CD117^{-/lo}$ $Fc\varepsilon RI^{+}$ cells after

335 culture, consistent with a basophil-like phenotype. Thus, CMPs$^{FcεRI+}$ exhibit a
336 considerable mast cell-forming capacity but also include constitute progenitors with
337 non-mast cell output. Basophils mature in bone marrow, whereas mast cells mature in
338 peripheral tissues, which likely explains why bone marrow CMPs$^{FcεRI+}$ form CD117^{-}
339 FcεRI^{+} basophil-like cells, whereas CD34^{+} CD117$^{int/hi}$ FcεRI^{+} blood progenitors do
340 not. The high frequency of CD117^{-} FcεRI^{+} basophil-like cells that develop from
341 CMPs$^{FcεRI+}$ is also in agreement with the reduced CD117 expression of CMPs$^{FcεRI+}$
342 compared with that of CMPs$^{FcεRI-}$. CD117 is upregulated upon mast cell maturation,
343 and blood mast cell progenitors express intermediate to high levels of CD117.
344 CMPs$^{FcεRI+}$ express CD117 at low levels overall, even though there are individual
345 CMPs$^{FcεRI+}$ cells that express high CD117 levels, which might correspond to the cells
346 with mast cell-forming capacity. Taken together, our results indicate that the low *KIT*
347 mutation prevalence in the CMP$^{FcεRI+}$ fraction is likely explained by the capacity of
348 these cells' to form not only mast cells but also CD117^{-} FcεRI^{+} basophil-like cells.
349
350 In SM, mast cells are known to aberrantly express multiple surface proteins, among
351 CD2 and CD25 are currently used for diagnosis.[35] These markers are expressed
352 independently of the SM subtype. Other markers, such as CD30 and CD52, are
353 associated with advanced SM and mast cell leukemia.[36,37] In the present study, we
354 demonstrate that CD45RA is a novel marker for aberrant mast cells in SM.
355 Remarkably, bone marrow mast cells from two patients with cutaneous mastocytosis
356 did not express CD45RA, suggesting that CD45RA is a specific marker for systemic
357 mast cell disease. Taken together, our results indicate that CD45RA expression should
358 be considered a novel marker for diagnosis of SM.
359

360 CD45RA is present on aberrant mast cells in SM, but at what stage during mast cell
361 differentiation is the marker upregulated? CMPs$^{FcεRI+}$, which lack CD45RA, present
362 mast cell-forming potential in SM patients. In contrast, we show that cells in the
363 classic CD45RA^{+} GMP gate lack mast cell potential in SM patients. An alternative
364 explanation is that the mast cell progenitors in SM fall into the immature CD38^{-} gate.
365 In fact, examples of rare mutated CD117$^{int/hi}$ FcεRI$^{int/hi}$ cells in the CD45RA^{+} LMPP
366 gate were seen (Figure S6C). It is also tempting to speculate that CD45RA is
367 upregulated once aberrant mast cells are mature.
368
369 The CD34^{+} HSPC population is highly heterogeneous and a single-cell resolution is
370 therefore necessary to delineate the cellular distribution of the mutation. Here, we
371 used single-cell index sorting to track cellular identity when performing mutation
372 analysis. Notably, the mutation was detected throughout differentiation, from HSCs to
373 the MEP, GMP, and LMPP fractions, depending on the patient. The detection of the
374 mutation in early HSPCs explains previous findings of the mutation being present in
375 bulk-sorted mature cell lineages of some patients.
376
377 Multiplex TaqMan qPCR assays detected the *KIT* mutation in index-sorted
378 progenitors in the present investigation. The qPCR method was originally developed
379 for sensitive mutation detection in DNA extracted from bone marrow or blood cells.
380 GAPDH primers and probes were added to the assay to confirm the presence or
381 absence of a sorted cell. This method allowed the detection of mutated cells with
382 close to 100% efficiency, with no observed false positives. The single-cell index
383 sorting and DNA mutation analysis approach can similarly be applied to other
384 mutations and hematologic diseases to reveal the origin of aberrant clones. One

385 limitation of the method is the number of cells that can be analyzed, meaning that
386 mutated cells in very rare subpopulations might go undetected. However, more than
387 10,000 HSPCs were analyzed in the present investigation, and single-cell index
388 sorting coupled with qPCR allowed unbiased and prospective analysis of mutated
389 HSPC populations in SM. Whole-genome amplification and nested PCR methods for
390 amplifying and sequencing DNA mutations from single cells are associated with the
391 phenomenon known as allelic dropout, which is the amplification of only a single
392 allele, leading to an overestimation of the frequency of non-mutated cells. Mutational
393 profiling of single colonies, as performed by Jawhar *et al*[18], avoids this problem.
394 However, such analysis can be performed only on progenitors that form sufficiently
395 large colonies. Mast cell progenitors present a poor proliferative capacity, and this
396 technique was therefore not applied in the present investigation.
397
398 In summary, we have explored the composition and mutation profile of $CD34^+$ HSPCs
399 from SM patients. The results show that the *KIT* mutation can be found in cells
400 throughout the hematopoietic landscape and exhibits accumulation in the mast cell
401 lineage, supporting the notion that the aberrant clone may arise in the hematopoietic
402 stem cell compartment. Furthermore, the mutated mast cells express CD45RA, a
403 potential novel clinical biomarker for aberrant mast cells in SM.
404
405 **Acknowledgements**
406 We wish to thank Kerstin Hamberg Levedahl for help with the patients. Stem cell
407 factor was a kind gift from SOBI, Stockholm, Sweden. This study was supported by
408 the Swedish Research Council, the Swedish Cancer Society, the Stockholm Cancer
409 Society (Radiumhemmets Forskningsfonder), Magnus Bergvall's Foundation, Tore

410 Nilsson's Foundation for Medical Research, the Karolinska Institutet, and through the
411 regional agreement on medical training and clinical research (ALF) between
412 Stockholm County Council and the Karolinska Institutet, and ALF-funding from
413 Uppsala University Hospital.
414

415 **Authorship**

416 J.G., J.S.D. and G.N. designed the experiments; J.G., E.R.H. and J.S.D. performed the
417 experiments; J.G. and M.E. processed the patient samples. J.S.U., M.K., R.M.A., S.S.
418 and M.M. provided patient samples and diagnosed patients; M.A. provided the ROSA
419 cell line. J.G. and J.S.D. analyzed the data and wrote the first draft of the paper; and
420 all authors reviewed the manuscript; and J.S.D. and G.N. designed and supervised the
421 study and secured funding.
422

423 Conflict-of-interest disclosure: The authors have declared that no conflict of interest
424 exists.
425
426

427 **References**

428

429 1. Dahlin JS, Hallgren J. Mast cell progenitors: origin, development and
430 migration to tissues. *Mol Immunol*. 2015;63(1):9-17.

431 2. Grootens J, Ungerstedt JS, Nilsson G, Dahlin JS. Deciphering the
432 differentiation trajectory from hematopoietic stem cells to mast cells. *Blood Advances*.
433 In press.

434 3. Irani AM, Nilsson G, Miettinen U, et al. Recombinant human stem cell factor
435 stimulates differentiation of mast cells from dispersed human fetal liver cells. *Blood*.
436 1992;80(12):3009-3021.

437 4. Kirshenbaum AS, Goff JP, Kessler SW, Mican JM, Zsebo KM, Metcalfe DD.
438 Effect of IL-3 and stem cell factor on the appearance of human basophils and mast
439 cells from CD34+ pluripotent progenitor cells. *J Immunol*. 1992;148(3):772-777.

440 5. Valent P, Spanblochl E, Sperr WR, et al. Induction of differentiation of human
441 mast cells from bone marrow and peripheral blood mononuclear cells by recombinant
442 human stem cell factor/kit-ligand in long-term culture. *Blood*. 1992;80(9):2237-2245.

443 6. Mitsui H, Furitsu T, Dvorak AM, et al. Development of human mast cells
444 from umbilical cord blood cells by recombinant human and murine c-kit ligand. *Proc*
445 *Natl Acad Sci U S A*. 1993;90(2):735-739.

446 7. Nagata H, Worobec AS, Oh CK, et al. Identification of a Point Mutation in the
447 Catalytic Domain of the Protooncogene C-Kit in Peripheral-Blood Mononuclear-Cells
448 of Patients Who Have Mastocytosis with an Associated Hematologic Disorder. *Proc*
449 *Natl Acad Sci U S A*. 1995;92(23):10560-10564.

450 8. Valent P, Akin C, Escribano L, et al. Standards and standardization in
451 mastocytosis: consensus statements on diagnostics, treatment recommendations and
452 response criteria. *Eur J Clin Invest*. 2007;37(6):435-453.

453 9. Valent P, Akin C, Metcalfe DD. Mastocytosis: 2016 updated WHO
454 classification and novel emerging treatment concepts. *Blood*. 2017;129(11):1420-
455 1427.

456 10. Arock M, Sotlar K, Akin C, et al. KIT mutation analysis in mast cell
457 neoplasms: recommendations of the European Competence Network on Mastocytosis.
458 *Leukemia*. 2015;29(6):1223-1232.

459 11. Kristensen T, Vestergaard H, Moller MB. Improved detection of the KIT
460 D816V mutation in patients with systemic mastocytosis using a quantitative and
461 highly sensitive real-time qPCR assay. *J Mol Diagn*. 2011;13(2):180-188.

462 12. Afonja O, Amorosi E, Ashman L, Takeshita K. Multilineage involvement and
463 erythropoietin-"independent" erythroid progenitor cells in a patient with systemic
464 mastocytosis. *Ann Hematol*. 1998;77(4):183-186.

465 13. Garcia-Montero AC, Jara-Acevedo M, Teodosio C, et al. KIT mutation in
466 mast cells and other bone marrow hematopoietic cell lineages in systemic mast cell
467 disorders: a prospective study of the Spanish Network on Mastocytosis (REMA) in a
468 series of 113 patients. *Blood*. 2006;108(7):2366-2372.

469 14. Kocabas CN, Yavuz AS, Lipsky PE, Metcalfe DD, Akin C. Analysis of the
470 lineage relationship between mast cells and basophils using the c-kit D816V mutation
471 as a biologic signature. *J Allergy Clin Immunol*. 2005;115(6):1155-1161.

472 15. Yavuz AS, Lipsky PE, Yavuz S, Metcalfe DD, Akin C. Evidence for the
473 involvement of a hematopoietic progenitor cell in systemic mastocytosis from single-
474 cell analysis of mutations in the c-kit gene. *Blood*. 2002;100(2):661-665.

475 16. Pardanani A, Reeder T, Li CY, Tefferi A. Eosinophils are derived from the
476 neoplastic clone in patients with systemic mastocytosis and eosinophilia. *Leuk Res*.
477 2003;27(10):883-885.

478 17. Mayado A, Teodosio C, Dasilva-Freire N, et al. Characterization of CD34(+)
479 hematopoietic cells in systemic mastocytosis: Potential role in disease dissemination.
480 *Allergy*. 2018;73(6):1294-1304.

481 18. Jawhar M, Schwaab J, Schnittger S, et al. Molecular profiling of myeloid
482 progenitor cells in multi-mutated advanced systemic mastocytosis identifies KIT
483 D816V as a distinct and late event. *Leukemia*. 2015;29(5):1115-1122.

484 19. Jara-Acevedo M, Teodosio C, Sanchez-Munoz L, et al. Detection of the KIT
485 D816V mutation in peripheral blood of systemic mastocytosis: diagnostic
486 implications. *Mod Pathol*. 2015;28(8):1138-1149.

487 20. Arber DA, Orazi A, Hasserjian R, et al. The 2016 revision to the World Health
488 Organization classification of myeloid neoplasms and acute leukemia. *Blood*.
489 2016;127(20):2391-2405.

490 21. Saleh R, Wedeh G, Herrmann H, et al. A new human mast cell line expressing
491 a functional IgE receptor converts to tumorigenic growth by KIT D816V transfection.
492 *Blood*. 2014;124(1):111-120.

493 22. Sundstrom M, Vliagoftis H, Karlberg P, et al. Functional and phenotypic
494 studies of two variants of a human mast cell line with a distinct set of mutations in the
495 c-kit proto-oncogene. *Immunology*. 2003;108(1):89-97.

496 23. Dahlin JS, Ekoff M, Grootens J, et al. KIT signaling is dispensable for human
497 mast cell progenitor development. *Blood*. 2017;130(16):1785-1794.

498 24. Harvima IT, Naukkarinen A, Harvima RJ, Fraki JE. Immunoperoxidase and
499 enzyme-histochemical demonstration of human skin tryptase in cutaneous mast cells
500 in normal and mastocytoma skin. *Arch Dermatol Res*. 1988;280(6):363-370.

501 25. Dahlin JS, Ungerstedt JS, Grootens J, et al. Detection of circulating mast cells
502 in advanced systemic mastocytosis. *Leukemia*. 2016;30(9):1953-1956.

503 26. Notta F, Doulatov S, Laurenti E, Poeppl A, Jurisica I, Dick JE. Isolation of
504 Single Human Hematopoietic Stem Cells Capable of Long-Term Multilineage
505 Engraftment. *Science*. 2011;333(6039):218-221.

506 27. Majeti R, Park CY, Weissman IL. Identification of a hierarchy of multipotent
507 hematopoietic progenitors in human cord blood. *Cell Stem Cell*. 2007;1(6):635-645.

508 28. Manz MG, Miyamoto T, Akashi K, Weissman IL. Prospective isolation of
509 human clonogenic common myeloid progenitors. *Proc Natl Acad Sci U S A*.
510 2002;99(18):11872-11877.

511 29. Goardon N, Marchi E, Atzberger A, et al. Coexistence of LMPP-like and
512 GMP-like leukemia stem cells in acute myeloid leukemia. *Cancer Cell*.
513 2011;19(1):138-152.

514 30. Lee J, Breton G, Oliveira TY, et al. Restricted dendritic cell and monocyte
515 progenitors in human cord blood and bone marrow. *J Exp Med*. 2015;212(3):385-399.

516 31. Olweus J, BitMansour A, Warnke R, et al. Dendritic cell ontogeny: a human
517 dendritic cell lineage of myeloid origin. *Proc Natl Acad Sci U S A*.
518 1997;94(23):12551-12556.

519 32. Doulatov S, Notta F, Eppert K, Nguyen LT, Ohashi PS, Dick JE. Revised map
520 of the human progenitor hierarchy shows the origin of macrophages and dendritic
521 cells in early lymphoid development. *Nat Immunol*. 2010;11(7):585-593.

522 33. Dahlin JS, Malinovschi A, Ohrvik H, et al. Lin- CD34hi CD117int/hi
523 FcepsilonRI+ cells in human blood constitute a rare population of mast cell
524 progenitors. *Blood*. 2016;127(4):383-391.

525 34. Gorgens A, Radtke S, Mollmann M, et al. Revision of the human
526 hematopoietic tree: granulocyte subtypes derive from distinct hematopoietic lineages.
527 *Cell Rep*. 2013;3(5):1539-1552.

528 35. Teodosio C, Mayado A, Sanchez-Munoz L, et al. The immunophenotype of
529 mast cells and its utility in the diagnostic work-up of systemic mastocytosis. *J Leukoc*
530 *Biol*. 2015;97(1):49-59.

531 36. Sotlar K, Cerny-Reiterer S, Petat-Dutter K, et al. Aberrant expression of CD30
532 in neoplastic mast cells in high-grade mastocytosis. *Mod Pathol*. 2011;24(4):585-595.

533 37. Hoermann G, Blatt K, Greiner G, et al. CD52 is a molecular target in
534 advanced systemic mastocytosis. *FASEB J*. 2014;28(8):3540-3551.
535

536 **Table legend**

537 **Table 1. Immunophenotypes of HSPCs**

538

539 **Figure legends**

540 **Figure 1. HSPC gating and profiling shows a normal course of hematopoiesis in**

541 **patients with systemic mastocytosis.** (A) A landscape model of the hematopoiesis.

542 (B) Gating strategy for bone marrow HSPCs and mature mast cells, showing

543 representative plots with population frequencies as percentages. (C) The

544 hematopoietic progenitor profile of 34 bone marrow samples. Cutaneous mastocytosis

545 samples are indicated in italics. (D) SM samples were compared with control samples

546 without SM, including CM (open circles), and the mean expression + SEM of each

547 HSPC is presented as a percentage of the total $CD34^{+}$ cells. The unpaired *t*-test was

548 used in panel D to compare the control and SM groups for each HSPC subset.

549

550 **Figure 2. The $CMP^{Fc\varepsilon RI+}$ fraction in the bone marrow has mast cell potential.** (A-

551 C) Flow cytometry analysis of cells cultured with rhIL-3 and rhIL-6 up to 21 days.

552 (A) Flow cytometry plots of representative cultures, showing the percentages of

553 $CD117^{-}$, $CD117^{+}$, and $CD117^{hi}$ cells in each plot. (B) Percentage of $CD117^{hi}$ $Fc\varepsilon RI^{+}$

554 cells at days 5-6 (n = 5). (C) Two of the samples in panel B were followed for up to

555 21 days under culture with rhIL-3 and rhIL-6. The percentage of $CD117^{hi}$ cells was

556 analyzed on days 5-6, 13-14, and 19-21. (D-E) Cells stained for enzymatic tryptase

557 and MGG after culturing with rhIL-3 and rhIL-6 for 5 days, followed by rhIL-6 and

558 SCF up to day 21 (n = 5). (D) Quantification of tryptase-positive cells at days 13-14

559 and 17-21 (n = 5). (E) Representative images of cultured $CMP^{Fc\varepsilon RI-}$ and $CMP^{Fc\varepsilon RI+}$

560 cells after 13-14 days, showing tryptase staining (red) and granules by May-Grünwald

561 Giemsa (MGG) staining. Samples Ctrl29, SM28, SM32, SM33, and MDS30 were
562 analyzed in panels B, D, and E. Samples SM32 and SM33 were analyzed in panels A
563 and C. The bars and lines in panel B, C and D represent the means ± SEM. The paired
564 t-test was used in panel B. $^{**}P < .01$. Images were captured using an Olympus XC10
565 camera (Olympus, Tokyo, Japan). The image width corresponds to 29 μm.
566
567 **Figure 3. SM mast cells aberrantly express CD45RA.** (A) Enzymatic staining
568 demonstrates tryptase expression, and MGG staining reveals granules in SM mast
569 cells. The images are representative of two experiments (samples SM32 and SM33).
570 Images were captured using an Olympus XC10 camera (Olympus, Tokyo, Japan). The
571 image width corresponds to 29 μm. (B) Mast cell frequencies in Ctrl, ISM, AdvSM,
572 and MDS/MPN patients, showing the median of log-transformed values. (C)
573 Histograms showing CD45RA expression in mast cells (red line), FMO controls (grey
574 histogram) and $CD34^{+}$ cells (dotted line). (D) Frequency of CD45RA-expressing mast
575 cells, showing the mean and SEM. Control subjects included two subjects with CM
576 (open circles). One-way ANOVA with Tukey's multiple comparison was used in
577 panels B and D, $^{*}P < .05$, $^{**}P < .01$, $^{****}P < .0001$.
578
579 **Figure 4. The percentage of mast cells in bone marrow correlates with clinical**
580 **features.** The percentage of mast cells was correlated with (A) serum tryptase levels
581 and (B) the percentage of BMMC infiltrate. (C) Serum tryptase levels were correlated
582 with the percentage of BMMC infiltrate. The samples include ISM (closed dots) and
583 AdvSM (open dots). Correlation values and significance are indicated in the figure
584 and in Table S2. Linear regression was calculated based on log-transformed data: in
585 panel A, n = 25, and in panels B and C, n = 23. The percentage of BMMC infiltrate

586 was not determined for two patients, accounting for the difference in numbers
587 between panels. For analytical purposes, BMMC infiltrate presented as <1% or <5%
588 in Table S1 were set at 1% and 5% respectively.
589
590 **Figure 5. Mutation analysis of KIT D816V in single cells identifies mutated**
591 **HSPCs and mast cells.** (A) Method of single-cell mutation analysis using index
592 sorting and multiplex qPCR. (B-C) The bars indicate the means + SEM percentage of
593 mutated cells for (B) mast cells and (C) HSPCs. (D) The cellular distribution of the
594 mutation in 10 different HSPCs, showing the total numbers of mutated and sorted
595 cells for each sample that passed the quality control procedure. (E) The bars indicate
596 the median percentage of mutated cells per HSPC. (F-G) Mutation frequencies of
597 selectively isolated HSPCs following a 2-step sorting protocol in two samples (SM28,
598 ISM; and SM31, AdvSM). These two samples are indicated with open circles in
599 panels B and E.
600
601 **Figure 6. The mutation rate in mast cells and HSPCs correlates with clinical**
602 **features.** (A-C) Linear regression of the percentage of mutated mast cells, showing
603 significant correlations with (A) the percentage of mast cells and (B) serum tryptase
604 levels. (C) The percentage of mutated HSPCs was correlated with serum tryptase
605 levels. The samples included ISM (closed dots) and AdvSM (open dots). Correlation
606 and significance are indicated in the figure and in Table S2. Linear regression was
607 calculated based on log-transformed data in panels A-C, n = 12 and D, n = 10.

Table 1. Immunophenotypes of hematopoietic stem and progenitor cells

Short	Cell type	Gating strategy	Reference
HSC	Hematopoietic stem cell	$CD14^{-}$ $CD34^{+}$ $CD38^{-}$ $CD45RA^{-}$ $CD90^{+}$	26, 27
MPP	Multipotent progenitor	$CD14^{-}$ $CD34^{+}$ $CD38^{-}$ $CD45RA^{-}$ $CD90^{-}$	26, 27
$CMP^{FcεRI-}$	Common myeloid progenitor $FcεRI^{-}$	$CD14^{-}$ $CD34^{+}$ $CD38^{+}$ $CD45RA^{-}$ $CD10^{-}$ $CD123^{+}$ $FcεRI^{-}$	28 *
$CMP^{FcεRI+}$	Common myeloid progenitor $FcεRI^{+}$	$CD14^{-}$ $CD34^{+}$ $CD38^{+}$ $CD45RA^{-}$ $CD10^{-}$ $CD123^{+}$ $FcεRI^{+}$ $CD117^{+}$	28 *
MEP	Megakaryocyte-erythroid progenitor	$CD14^{-}$ $CD34^{+}$ $CD38^{+}$ $CD45RA^{-}$ $CD10^{-}$ $CD123^{-}$	28
LMPP	Lymphoid-primed multipotent progenitor	$CD14^{-}$ $CD34^{+}$ $CD38^{-}$ $CD45RA^{+}$	29
GMP	Granulocyte-monocyte progenitor	$CD14^{-}$ $CD34^{+}$ $CD38^{+}$ $CD45RA^{+}$ $CD10^{-}$ $CD123^{+}$	28
CDP	Common dendritic progenitor	$CD14^{-}$ $CD34^{+}$ $CD38^{+}$ $CD45RA^{+}$ $CD10^{-}$ $CD123^{hi}$	30, 31
MLP	Multilymphoid progenitor	$CD14^{-}$ $CD34^{+}$ $CD38^{-}$ $CD45RA^{+}$ $CD10^{+}$	32
BNKP	B- and NK cell progenitor	$CD14^{-}$ $CD34^{+}$ $CD38^{+}$ $CD45RA^{+}$ $CD10^{+}$	32
MC	Mast cell	$CD14^{-}$ $CD34^{-}$ $CD117^{hi}$ $FcεRI^{+}$	

* Refers to the original CMP population without the inclusion of the FcεRI marker.

Figure 1

A

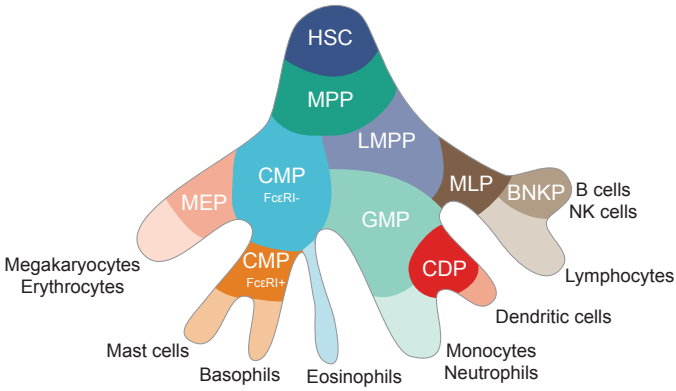

B

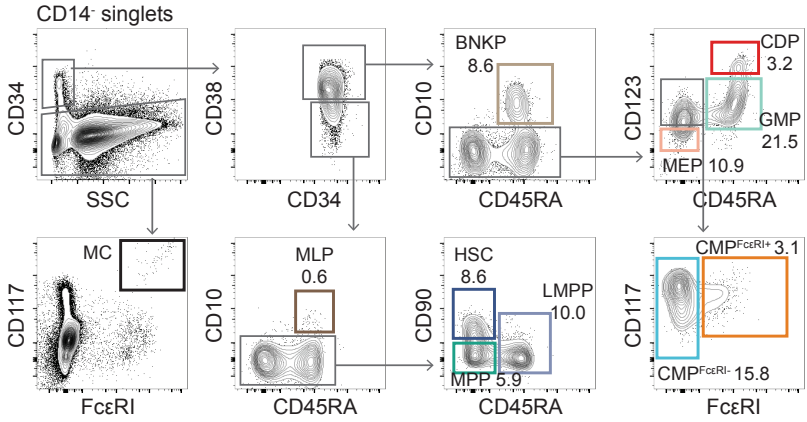

C

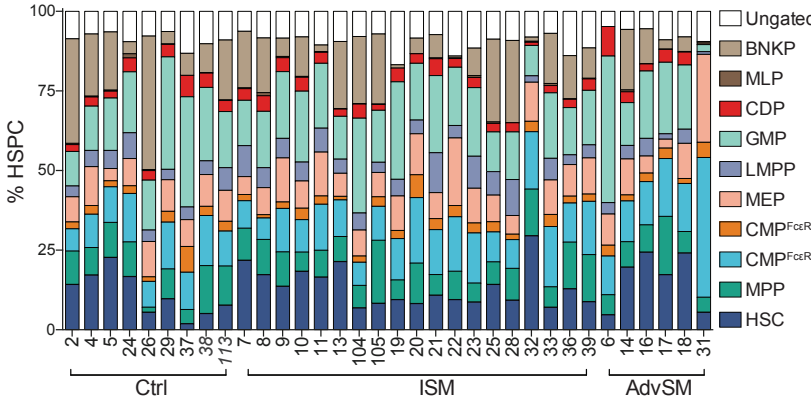

D

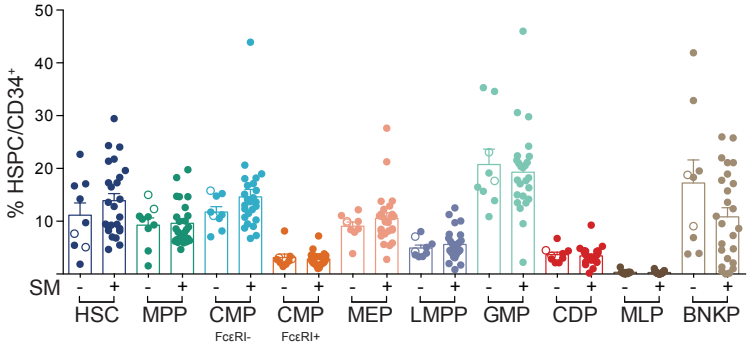

Figure 2

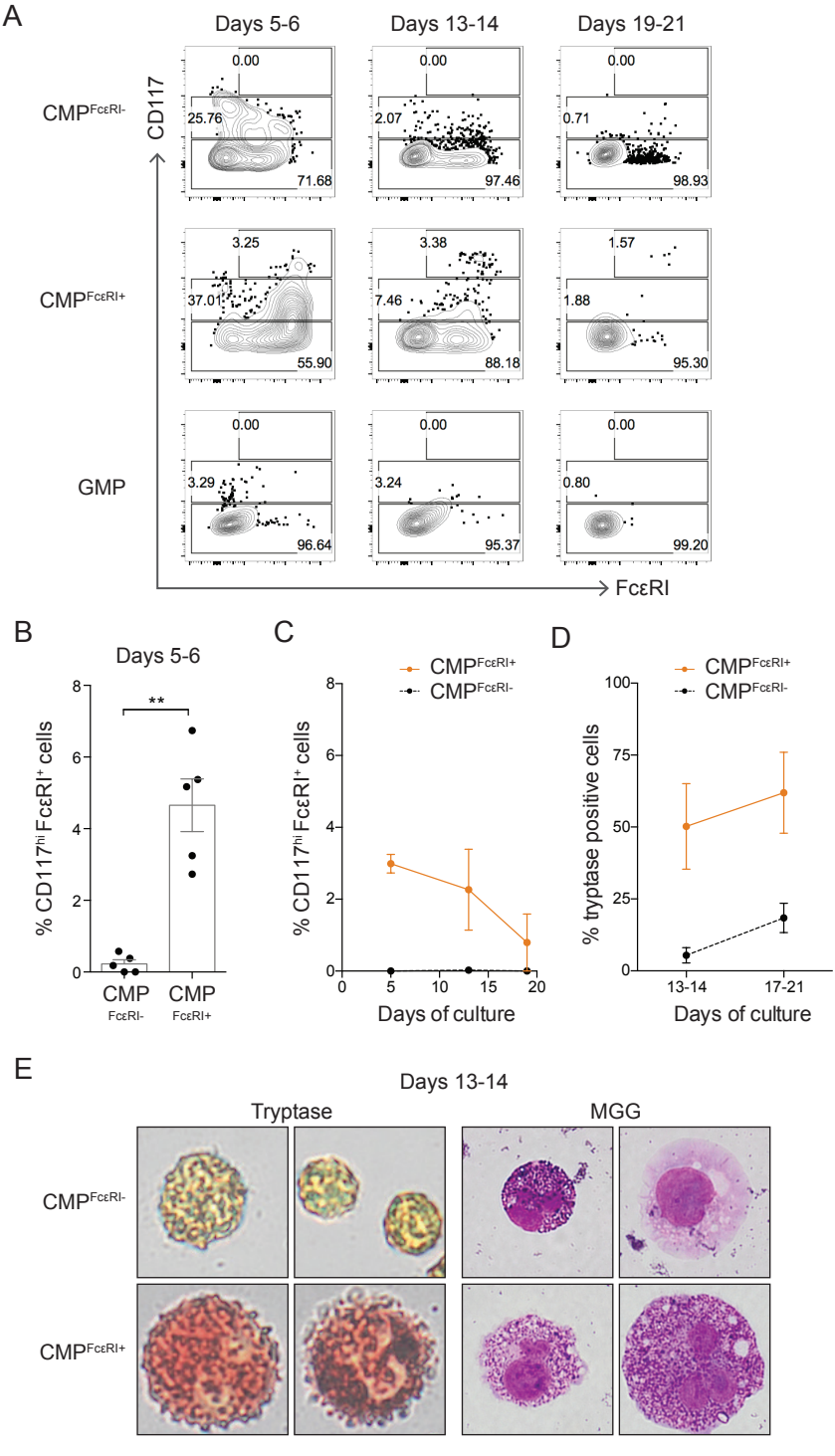
A
Days 5-6
Days 13-14
Days 19-21
CD117
FcεRI
CMPFcεRI-
CMPFcεRI+
GMP
0.00
25.76
71.68
0.00
2.07
97.46
0.00
0.71
98.93
3.25
37.01
55.90
3.38
7.46
88.18
1.57
1.88
95.30
0.00
3.29
96.64
0.00
3.24
95.37
0.00
0.80
99.20
B
Days 5-6
% CD117hi FcεRI+ cells
**
CMP FcεRI-
CMP FcεRI+
C
CMPFcεRI+
CMPFcεRI-
% CD117hi FcεRI+ cells
Days of culture
D
CMPFcεRI+
CMPFcεRI-
% tryptase positive cells
13-14
17-21
Days of culture
E
Days 13-14
Tryptase
MGG
CMPFcεRI-
CMPFcεRI+

Figure 3

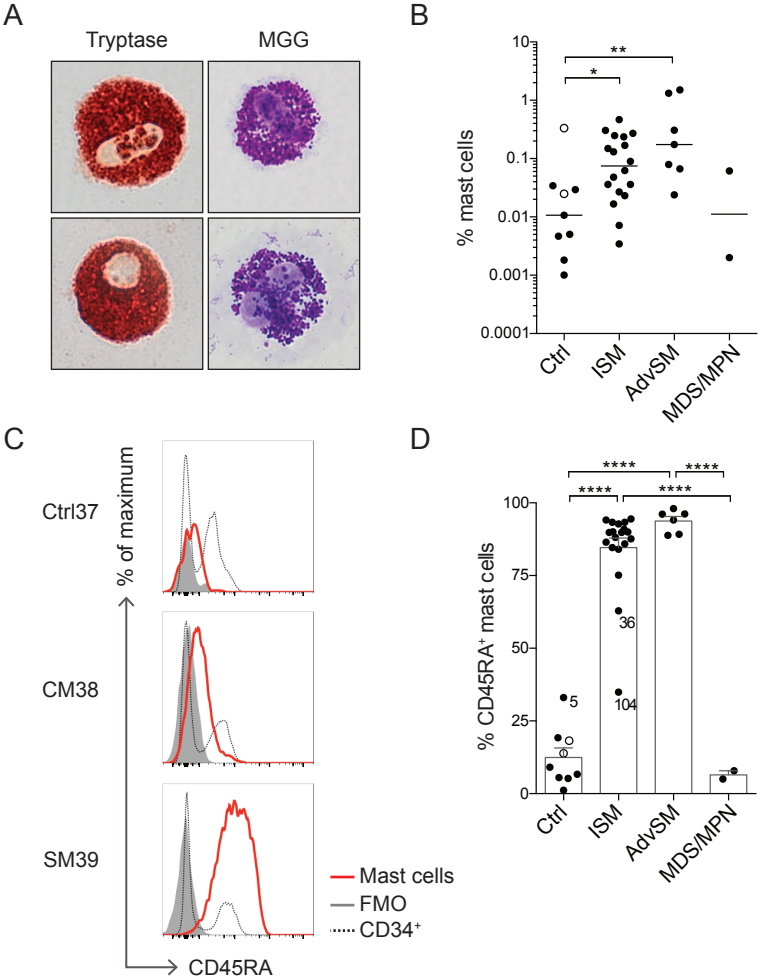
A
Tryptase
MGG
B
% mast cells
10
1
0.1
0.01
0.001
0.0001
**
*
Ctrl
ISM
AdvSM
MDS/MPN
C
% of maximum
Ctrl37
CM38
SM39
CD45RA
Mast cells
FMO
CD34+
D
% CD45RA+ mast cells
100
75
50
25
0
****
****
****
****
5
36
104
Ctrl
ISM
AdvSM
MDS/MPN

Figure 4

A

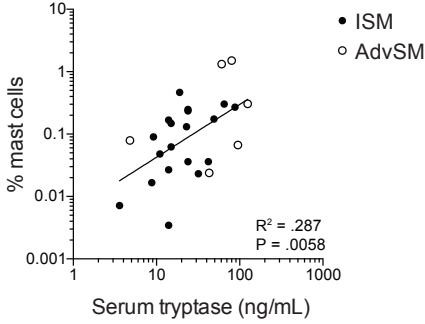
ISM
AdvSM
% mast cells
10
1
0.1
0.01
0.001
1
10
100
1000
Serum tryptase (ng/mL)
R² = .287
P = .0058

B

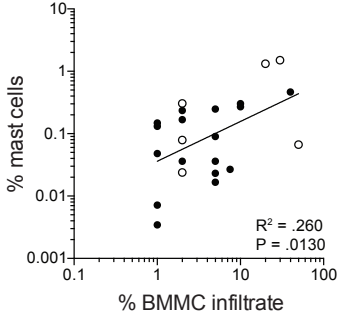
% mast cells
10
1
0.1
0.01
0.001
0.1
1
10
100
% BMMC infiltrate
R² = .260
P = .0130

C

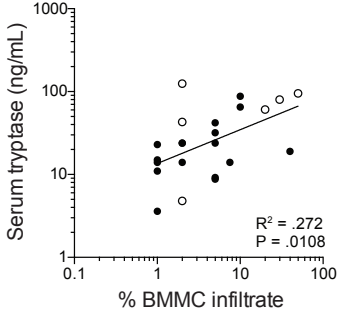
Serum tryptase (ng/mL)
1000
100
10
1
0.1
1
10
100
% BMMC infiltrate
R² = .272
P = .0108

Figure 5

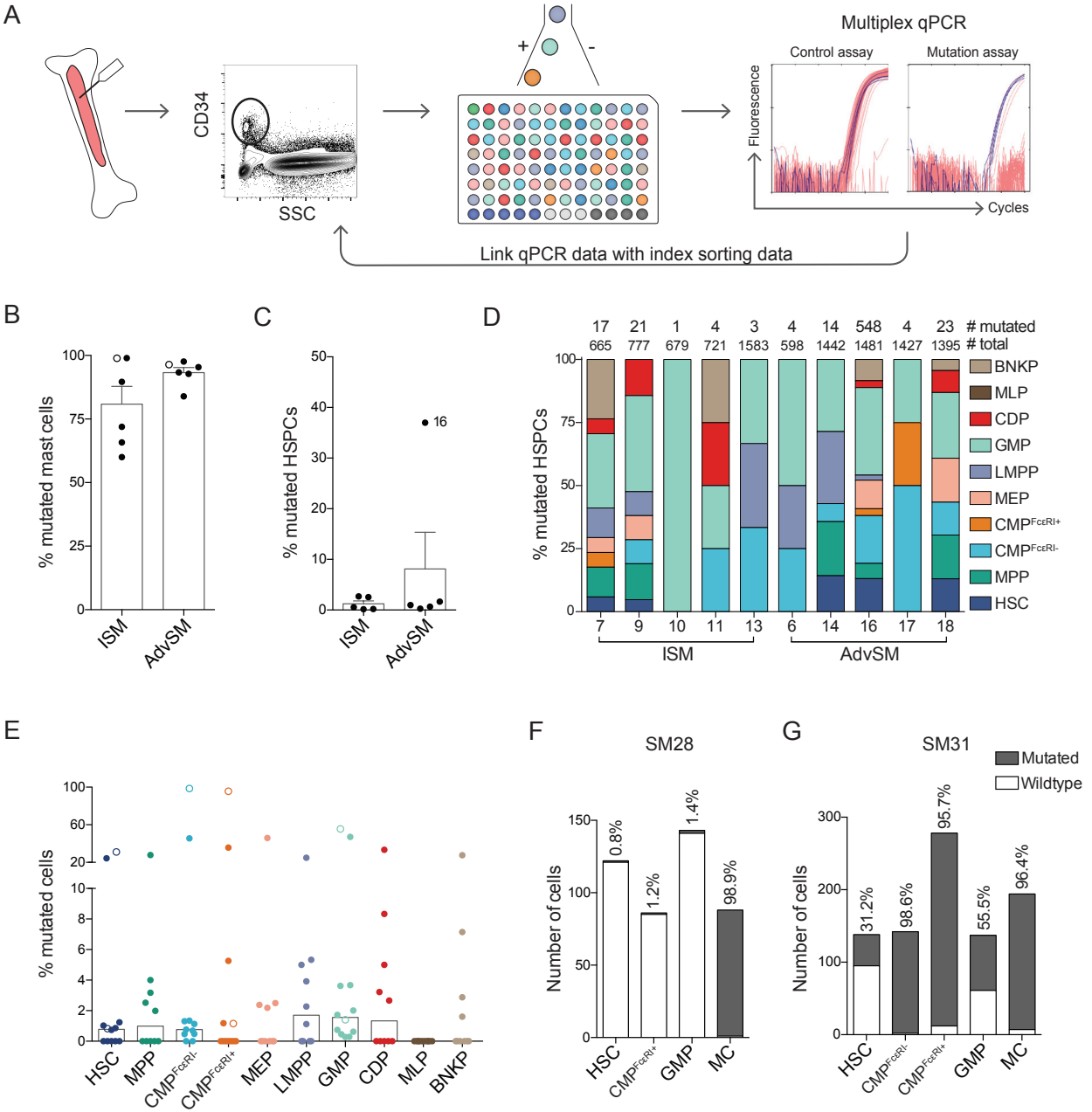
A
CD34
SSC
+
-
Multiplex qPCR
Control assay
Mutation assay
Fluorescence
Cycles
Link qPCR data with index sorting data
B
% mutated mast cells
ISM
AdvSM
C
% mutated HSPCs
16
ISM
AdvSM
D
mutated
total
17 21 1 4 3 4 14 548 4 23
665 777 679 721 1583 598 1442 1481 1427 1395
% mutated HSPCs
BNKP
MLP
CDP
GMP
LMPP
MEP
CMP^FcεRI+
CMP^FcεRI-
MPP
HSC
7 9 10 11 13 6 14 16 17 18
ISM
AdvSM
E
% mutated cells
HSC
MPP
CMP^FcεRI-
CMP^FcεRI+
MEP
LMPP
GMP
CDP
MLP
BNKP
F
SM28
Number of cells
0.8%
1.2%
1.4%
98.9%
HSC
CMP^FcεRI+
GMP
MC
G
SM31
Mutated
Wildtype
Number of cells
31.2%
98.6%
95.7%
55.5%
96.4%
HSC
CMP^FcεRI-
CMP^FcεRI+
GMP
MC

Figure 6

A

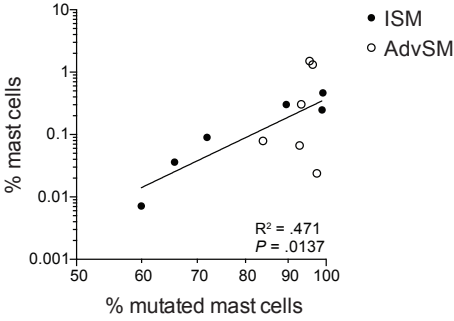
ISM
AdvSM
% mast cells
10
1
0.1
0.01
0.001
50
60
70
80
90
100
% mutated mast cells
R² = .471
P = .0137

B

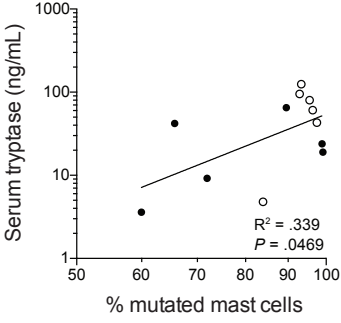
Serum tryptase (ng/mL)
1000
100
10
1
50
60
70
80
90
100
% mutated mast cells
R² = .339
P = .0469

C

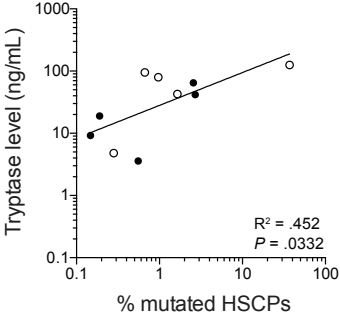
Tryptase level (ng/mL)
1000
100
10
1
0.1
0.1
1
10
100
% mutated HSCPs
R² = .452
P = .0332